FULL PAPER

# Metal–Insulator–Semiconductor Coaxial Microfibers Based on Self-Organization of Organic Semiconductor:Polymer Blend for Weavable, Fibriform Organic Field-Effect Transistors

*Hae Min Kim, Hyun Wook Kang, Do Kyung Hwang, Ho Sun Lim, Byeong-Kwon Ju, and Jung Ah Lim**

**With the increasing importance of electronic textiles as an ideal platform for wearable electronic devices, requirements for the development of functional electronic fibers with multilayered structures are increasing. In this paper, metal–polymer insulator–organic semiconductor (MIS) coaxial microfibers using the self-organization of organic semiconductor:insulating polymer blends for weavable, fibriform organic field-effect transistors (FETs) are demonstrated. A holistic process for MIS coaxial microfiber fabrication, including surface modification of gold microfiber thin-film coating on the microfiber using a die-coating system, and the self-organization of organic semiconductor–insulator polymer blend is presented. Vertical phase-separation of the organic semiconductor:insulating polymer blend film wrapping the metal microfibers provides a coaxial bilayer structure of gate dielectric (inside) and organic semiconductor (outside) with intimate interfacial contact. It is determined that the fibriform FETs based on MIS coaxial microfiber exhibit good charge carrier mobilities that approach the values of typical devices with planar substrate. It additionally exhibits electrical property uniformity over the entire fiber surface and improved bending durability. Fibriform organic FET embedded in a textile is demonstrated by weaving MIS coaxial microfibers with cotton and conducting threads, which verifies the feasibility of MIS coaxial microfiber for use in electronic textile applications.**

## 1. Introduction

With the recent demand for smart wearable electronic devices, the electrical textile (e-textile) has garnered considerable attention as an ideal device platform on account of its light weight, flexibility, and comfort for wearing. Compared with conventional thin-film-based electronic devices, e-textile electronic devices are integrated into the fiber itself or built into the fabric by weaving the functional electronic fibers. To date, many research groups have shown the feasibility of e-textile structures in various applications in supercapacitors,[1–3] sensors,[4–6] energy harvesting[7,8] and storage devices,[9,10] light-emitting diodes,[11–14] and transistors.[15–24] It has been shown that developing electronic materials with fibrous structure and a multilayered assembly are critical for realizing e-textile-based wearable devices. Among various electronic devices, the fibriform transistor is a key component for organizing the electronic circuit in a textile platform. Two types of fiber-based transistors with different operation principles have been demonstrated: The electrochemical transistor[15–19] and field-effect transistor.[20–24] The former devices were fabricated by creating junctions using two conducting fibers and adding an electrolyte lump at the junction of the fibers. Although this type of transistor is relatively easy to fabricate, critical drawbacks include fiber dislocation by mechanical deformation and a long response time, which can be problematic for practical use.[25] In comparison, field-effect transistors (FETs) based on a multilayered thin-film structure of conducting electrodes, an insulator, and a semiconductor exhibited good electrical performance and mechanical compatibility for a flexible substrate. In particular, organic FETs (OFETs) comprised of organic or polymeric electronic materials have been shown to be a promising component for e-textile applications on account of their flexibility, light weight, and ease of implementation. However, fiber-based OFET is

H. M. Kim, Dr. D. K. Hwang, Dr. J. A. Lim
Korea Institute of Science and Technology
Hwarangno 14-gil 5, Seongbuk-gu
Seoul 02972, South Korea
E-mail: jalim@kist.re.kr
H. M. Kim, Prof. B.-K. Ju
Department of Electrical Engineering
Korea University
Anam-ro, Seongbuk-gu
Seoul 02841, South Korea
Prof. H. W. Kang
Department of Mechanical Engineering
Chonnam National University
Yongbongno, Buk-gu, Gwangju 61186, South Korea
Prof. H. S. Lim
Department of Chemical and Biological Engineering
Sookmyung Women's University
Cheongpa-ro 47-gil 100, Seoul 04310, South Korea

DOI: 10.1002/adfm.201504972

still challenging because charge transport in OFETs is very sensitive to thin-film properties including the interfacial properties of gate insulator and organic semiconductor, surface roughness of the substrate, and molecular orientation of organic semiconductors.

In previous reports, OFETs fabricated on metallic single fiber were demonstrated by using vacuum-deposited metal-oxide dielectrics and organic semiconductors.[20,21] However, these devices showed poor bending durability and electrical performance compared with planar OFETs with the same device configuration owing to the rough interface of metallic fiber substrate. More recently, Jang et al. reported cylindrical OFETs with high bending stability. The electropolishing of aluminium wire and coating of the polymer dielectric layer on the wire improved the roughness of the metal wire surface.[23] However, the demonstrated fiber-based OFETs were only built on one side of the fiber using vacuum deposition of the semiconductor and electrode layer. This approach is limited for integrating them into the textile with conducting interconnects. Furthermore, fabrication of fibriform OFETs using a simple solution coating of organic thin layers has not been demonstrated until now. To make the fibriform OFETs practical, metal–insulator–semiconductor coaxial fibers with smooth interfaces, and organic semiconductor thin-films with controlled molecular orientation via a facile solution process, should be developed.

Here, we propose a simple strategy for the fabrication of metal-polymer insulator-organic semiconductor (MIS) coaxial microfibers for realization of weavable fibriform OFETs. The strategy is initiated with a surface modification of metal microfiber to improve the wettability of the polymer solution in the coating process and the interface adhesion of the coated thin-films on the microfibers. In particular, we utilize vertical phase-separation of organic semiconductor:insulating polymer blends to obtain homogeneously coated coaxial bilayers of insulating polymer (inside) and organic semiconductor (outside) thin-films on the metal microfiber surface. In previous works, we successfully demonstrated OFET devices based on vertical phase-separation of organic semiconductor:insulating polymer blends, whereby separate functional layers of the semiconductor and gate insulator or semiconductor and the top passivation layer in the OFET device were deposited in a one-step film deposition process.[26–28] This is a promising approach for fabricating MIS coaxial microfibers because the excellent film-forming properties inherent with polymer component facilitates coating of the thin-films on the microfiber as well as formation of the intimate interface between the dielectric and semiconductor layers which is critical for the achievement of transistor performance. In this work, demonstrated fibriform transistor based on the MIS coaxial microfiber showed good electrical performance comparable to that of typical devices fabricated on planar substrate. It was confirmed that the electrical performances of the MIS coaxial microfiber over the entire fiber surface were almost identical. Finally, the fibriform OFET was successfully integrated into fabric by weaving MIS coaxial microfibers with cotton and conducting threads as source and drain electrodes.

## 2. Results and Discussion

### 2.1. Fabrication and Characterization of MIS Coaxial Microfiber

**Figure 1** presents a holistic process for the fabrication of MIS coaxial microfibers based on organic semiconductor:insulating polymer blend. The process involves surface modification of the Au microfiber, die-coating of the polymer blend solution, and annealing of the coated blend film for leading vertical phase-separation and crystallization of the organic semiconductor. The Au microfiber with a 100-μm diameter was used as the core fiber substrate, which also served as a gate electrode of the FET device. Because the Au microfiber surface had poor surface wettability and interfacial adhesion, the surface modification was needed. In this work, mussel-inspired polydopamine (pDA) surface-adherent polymer was demonstrated as a surface modification layer of the Au microfiber. pDA is a promising material because the surface coating on a wide variety of substances can be achieved through a simple dip-coating process, and it can effectively change the surface characters of the substances to be hydrophilic.[29,30]

Simple immersion of the Au microfibers in an aqueous solution of dopamine resulted in spontaneous coating of the pDA film covering the fibers. Although a very thin layer (<10 nm) of pDA was formed on the Au surface, the decrease in the water contact angle on the Au surface from 70° to 33° after pDA coating clearly indicates that the wettability of the Au surface changed to be more hydrophilic by the pDA coating (Figure S1, Supporting Information). **Figure 2** exhibits cross-sectional and top scanning electron microscopy (SEM) images of Au microfibers coated by the thin polymer films through the die-coating method. Compared to the use of a pristine Au microfiber (Figure S2, Supporting Information), the pDA-treated Au microfiber shows good film adhesion without the films being peeled off (Figure 2a). Furthermore, surface modification of the Au microfiber by the pDA coating additionally improves the vertical phase-separation in the blend films coated on the Au microfibers. (A detailed explanation of phase-separation of the polymer blend film is discussed further below.)

For uniform coating of polymer thin-films on the Au microfiber, a die-coating system was developed (Figure 1). The pDA-treated Au microfiber passed through the T-shaped glass tube as a reservoir in which the polymer blend solution was continuously supplied from the syringe to fill inside the tube. The polymer solution was entrained by drawing of the fiber. The coated thin polymer layer was then dried by the heating unit next to the coating unit. In previous reports, coating of functional materials on fibers was performed using a dip-coating method.[11,23] However, nonuniform film coating, like a pearl necklace, can commonly occur in the dip-coating process (Figure S3, Supporting Information). Fluid coating on fiber is governed by various parameters, such as the fluid viscosity, coating velocity, solution meniscus, and solvent drying condition.[31] Compared to the dip-coating method, the die-coating system is beneficial for controlling the coating meniscus by varying the diameter of the tube, the fiber drawing speed, and the drying temperature of the heating unit.[5] In the proposed die-coating system, the thickness of coated film ($t$) on Au microfibers was controlled from

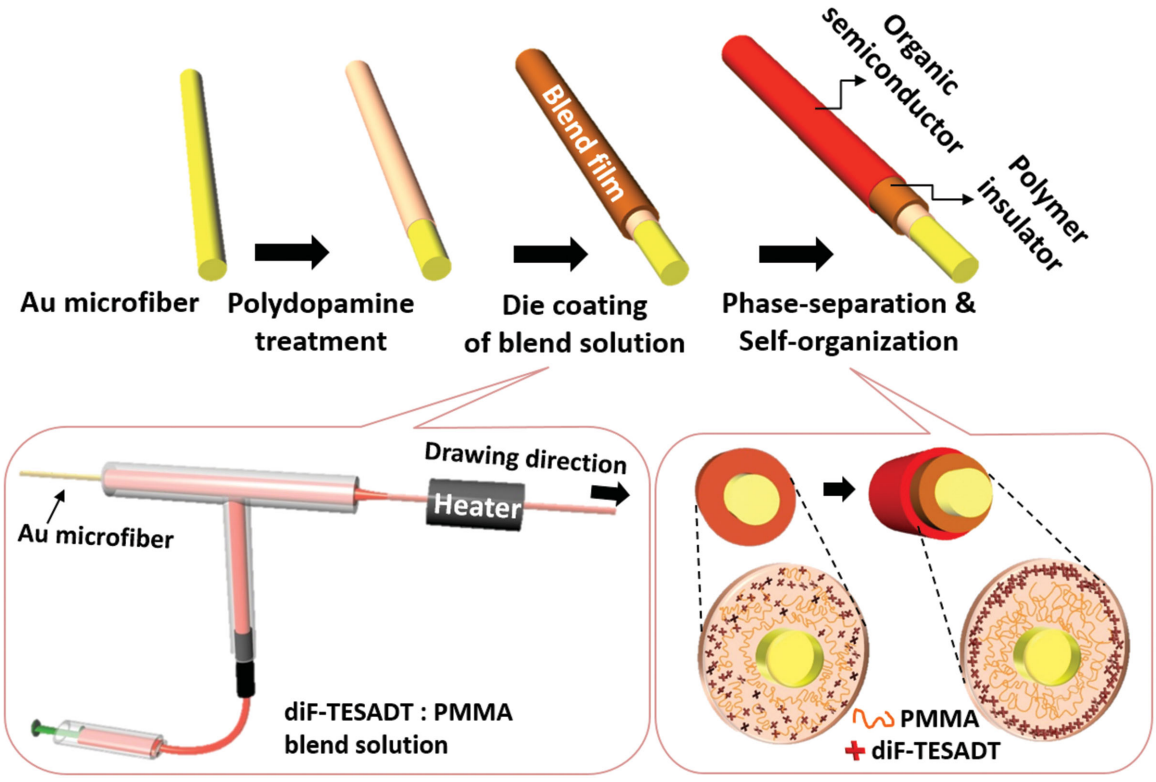


**Figure 1.** Schematic illustration for fabrication procedure of MIS microfibers with polymer insulator/organic semiconductor coaxial structure.

85 to 650 nm by varying the coating velocity of the microfiber ($v$) from 10 to 110 mm min$^{-1}$ (Figure 2b). It is notable that the plot of coating thickness versus the coating velocity exhibited two distinct regimes. One is that $t$ increased with each increment of $v$. In the other regime, on the other hand, $t$ decreased as $v$ increased. It is known that the coating thickness relates to the relationship between viscous forces and flows due to capillarity, which is known as Landau, Levich, and Derjaguin (LLD) equation, whereby the coated thickness is $(t) = 1.34Ca^{\frac{2}{3}}$ when $Ca \ll 1$. $Ca$ denotes the capillary number $Ca = \frac{\eta U}{\gamma}$, where $U$ is the coating velocity, $\gamma$ is the interfacial tension, and $\eta$ is the fluid viscosity.[31–33] At low-fiber coating velocity (under 70 mm min$^{-1}$ in this work), inertia driven by the fiber drawing can be neglected, and the coated thickness can be determined by the balance

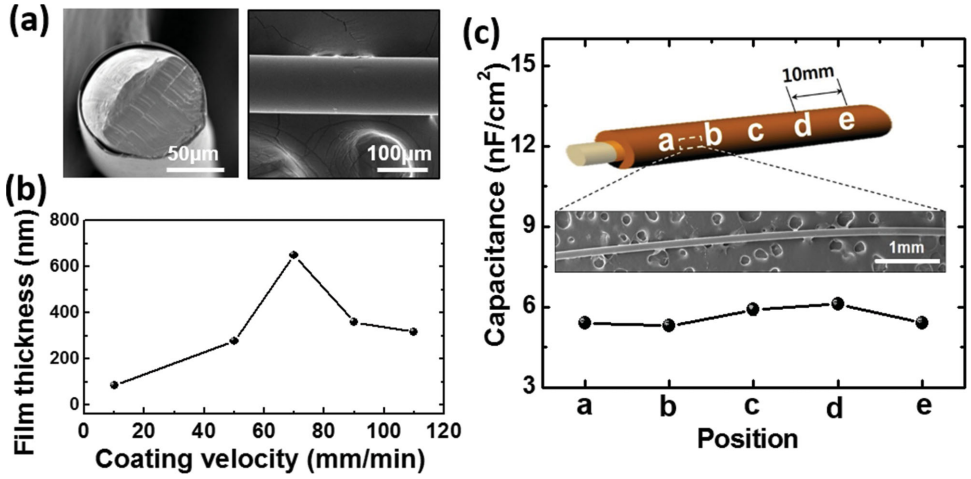


**Figure 2.** a) Cross-sectional and top SEM images of PMMA coated on pDA-treated Au microfiber. b) Film thickness of the coated blend film with respect to the variation in the coating velocity. c) The capacitance ($C_i$) values of PMMA dielectric layer after selective etching of diF-TESADT outside layer of the blend film wrapping the Au microfiber along the longitudinal direction. The inset of (c) illustrates a schematic representation of the measurement positions with a 10-mm interval and a top SEM image showing homogeneous coating of the film on the microfiber.

between the capillarity and viscosity given by the LLD equation. However, at a high coating velocity (higher than 70 mm $min^{-1}$), inertia becomes more important, and the layer entrained in the volume is the viscous boundary layer of thickness $\delta$ given by balancing the acceleration of the fluid with viscous force as $\delta \approx \sqrt{\frac{\eta L}{\rho V}}$, where $\rho$ is the solution density and $L$ is the length of the reservoir. In this regime, the coated thickness instead decreases as the coating velocity increases.[31] Ultimately, the developed die-coating method successfully provides highly uniform thin polymer film on the microfiber in a longitudinal direction, as shown in Figure 2c. To confirm the thickness uniformity of the polymer layer over the entire microfiber, the capacitance ($C_i$) at five different points with a regular interval (10 mm) along the microfiber was measured after selective dissolution of organic semiconductor. The relationship between $C_i$, permittivity of free space ($\varepsilon_0$), the relative permittivity ($\varepsilon_r$, poly(methyl methacrylate) (PMMA) = 2.8), the area of overlap of the metal ($A$), and dielectric film thickness ($t$) is given as $C_i = \varepsilon_0 \varepsilon_r A / t$. Consequently, almost all measured capacitances were nearly the same value of 5.62 ± 0.34 nF $cm^{-2}$ along the microfiber, which indicates that highly uniform polymer films were deposited on the microfibers by the die-coating method.

### 2.2. Self-Organization of Polymer Dielectric/Organic Semiconductor

After die-coating of the organic semiconductor:insulating polymer blend on the pDA-treated Au microfiber, vertical phase-separation of the blend film was induced to form the bilayers of polymer dielectric (inside) and organic semiconductor (outside) on the microfiber. Vertical phase-separation of 2,8-difluoro-5,11-bis(triethylsilylethynyl)anthradithiophene (diF-TESADT) and PMMA blend was utilized as a blend system for MIS coaxial microfibers. In previous work, we found that vertically phase-separated diF-TES ADT:PMMA blend film served the diF-TESADT channel at the top surface and the PMMA gate dielectric near the bottom substrate. This resulted in FET devices with good electrical performances.[28] An important issue of using this blend film in the OFET device is that blend film should be fully phase-separated in a vertical direction. In addition, organic semiconductor molecules in the vertically segregated film should be highly crystallized because the charge transport in the organic semiconductor is dependent on the molecular ordering and crystallinity of the film.[27,28,34] To enhance the crystallization of diF-TESADT molecules in the blend film, solvent vapor annealing (SVA) using 1,2-dichloroethane was successfully demonstrated. In the SVA process, the absorbed solvent molecules serve as a plasticizer and provide an environment in which the diF-TESADT molecules can easily move toward the air/film surface to minimize the surface energy and crystallize by strong intermolecular π–π interaction.[27]

**Figure 3**a indicates a schematic diagram of molecular assembly in the diF-TESADT/PMMA films wrapping the Au microfiber. Figure 3b shows optical microscope (OM) and polarized optical microscope (POM) images of the diF-TESADT:PMMA blend (1:4 weight ratio) film wrapping the Au microfibers. Immediately after die-coating the diF-TESADT:PMMA blend solution, a small amount of diF-TESADT microcrystals is sparsely distributed on the fiber surface. However, after the blend film-coated microfibers are exposed to the 1,2-dichloroethane vapor, the surface of the microfiber is covered by the diF-TESADT microcrystals with a lateral size of several tens micrometer in width, as shown in Figure 3b. These crystalline structures clearly originated from the crystallization of diF-TESADT because the atactic PMMA has an amorphous nature. Arrangement of microcrystals toward the fiber-drawing direction is not observed. After selective dissolution of diF-TESADT using cyclohexane, the shiny crystalline domain observed under polarized light disappeared and only the smooth polymer layer remained (Figure S4, Supporting Information). This implies that the coaxial bilayer structure of PMMA (inside) and diF-TESADT (outside) wrapping the Au microfiber was successfully constructed through the vertical phase-separation and crystallization of diF-TESADT molecules via the SVA process. To the best of our knowledge, this is the first demonstration that organic semiconductor:insulating polymer blend can be applied to the fibrous substrate, which provides a facile strategy for the preparation of the coaxial bilayer on the microfiber from a one-step coating process.

According to the previous study, surface energy of the blending components and interaction with the substrate surface are important factors affecting the phase-separation behavior of the polymer blend.[27,35] pDA treatment of the Au microfiber can influence the phase-separation of the diF-TESADT:PMMA blend film deposited on the microfiber. As shown in Figure 3c, OM images clearly show that, when the Au microfiber is treated by pDA, the diF-TESADT microcrystals cover most of the microfiber surface. To clarify the distribution of the PMMA and diF-TESADT in the blend film, a time of flight secondary ion mass spectroscopy (TOF-SIMS) combined with the local cesium ion beam sputtering was performed. The O- and F-peaks originated from the PMMA and diF-TESADT, respectively. 3D rendered overlay images of O-(blue) and F-(red) atoms clearly show that the top layer predominantly consists of diF-TESADT, and PMMA is located near the substrate. In particular, on the pDA-treated surface, the vertical phase-separation with a clear layer boundary is observed. This may be due to the preferential wetting of the PMMA component on the pDA surface. PMMA commonly wets the hydrophilic surface on account of the strong interaction between carbonyl groups of PMMA and the hydroxyl groups on the hydrophilic surface.[36] After selective removal of the top diF-TESADT layer using cyclohexane, we found that the PMMA dielectric layer wrapping the Au microfiber did not undergo dielectric breakdown until 100 V, which corresponds to a breakdown field of 3.1 MV $cm^{-1}$ (Figure S5, Supporting Information). This indicates that the phase-separated PMMA layer can successfully function as a bottom gate dielectric layer.

Morphological development of diF-TESADT:PMMA blend film was also investigated by varying the thickness of the blend film to optimize the MIS microfiber. The film thickness was controlled by varying the coating velocity in a die-coating process. As shown in Figure S6 in the Supporting Information, when the film thickness is ≈400 nm, large diF-TESDAT crystalline structures develop on the microfiber surface, where the thickness of the segregated diF-TESADT layer is ≈80 nm. At a thickness lower than 400 nm, small microcrystals of diF-TESADT are sparsely observed. This may be due

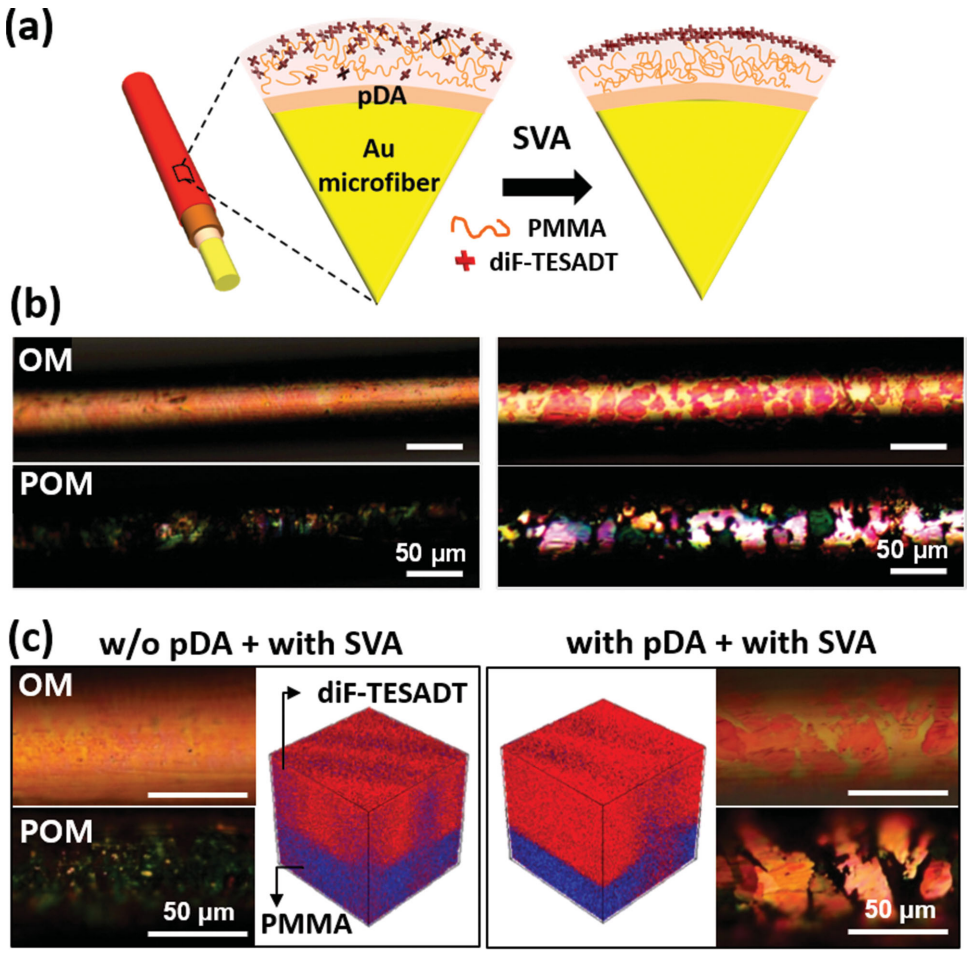


**Figure 3.** a) Schematic representations of phase-separation in the diF-TESADT/PMMA films before and after solvent vapor annealing (SVA). b) Optical microscope (OM) and polarized optical microscope (POM) images of PMMA/diF-TESADT blend film wrapping on Au microfiber before (left) and after (right) SVA. c) Comparison in OM (top)/POM (bottom) images and 3D rendered overlay images of O-(blue) and F-(red) distributions analyzed by TOF-SIMS for SVA-treated PMMA/diF-TESADT blend film on the microfiber according to the pDA treatment.

to an insufficient amount of diF-TESADT molecules to cover the entire film surface. On the other hand, in the thick blend film, penetration of solvent molecules throughout the whole film thickness could be limited in the SVA process. This might restrict the segregation of the diF-TESADT molecules located deep inside the film toward the film surface, resulting in a small domain size of microcrystals. In fact, it is observed that the MIS microfiber with a highly crystalline diF-TESADT structure (in a 400-nm-thick blend film) exhibits the highest charge carrier mobility when applied to the fibriform transistor.

### 2.3. Electrical Characteristics of MIS Coaxial Fiber

To evaluate the electrical performance of the MIS coaxial microfibers, fibriform OFETs with a top-contact configuration were fabricated by adding Au source and drain electrodes via thermal evaporation. A schematic diagram of the cross-sectional OFET structure and top-view OM/POM images of the fibriform transistor are shown in **Figure 4**a. **Table 1** lists the detailed device electrical properties for the fibriform transistors according to the pDA treatment and solvent vapor annealing. The field-effect mobility was calculated from the transfer curves of 30 devices. Without using pDA treatment or solvent vapor annealing, the device exhibits low field-effect mobility ($0.04 \pm 0.03$ cm$^2$ V$^{-1}$ s$^{-1}$) and an on/off current ratio, which may be attributed to the poor coating quality, incomplete phase-separation, and low crystallinity of the segregated diF-TESADT molecules. As shown in Figure 4b,c, the device based on the pDA-treated Au microfiber exhibits increased drain current ($I_{ds}$) and an improved on/off current ratio. The enhanced phase-separation of diF-TESADT:PMMA blend film on the pDA-treated Au surface results in this improvement. With the pDA modification of Au microfiber and solvent vapor annealing, a significant improvement is achieved in device performance, with the average mobility of $0.19 \pm 0.07$ cm$^2$ V$^{-1}$ s$^{-1}$ (the best mobility is 0.30 cm$^2$ V$^{-1}$ s$^{-1}$) and an $I_{on}/I_{off}$ current ratio of $\approx 10^4$, and no hysteresis during the gate voltage sweep. This performance closely approaches the values of the previously reported device built on planar substrates using polymer dielectric/organic semiconductor blends.[28,34,37] The crossover of the output characteristics at low gate bias is due to the gate leakage, which can

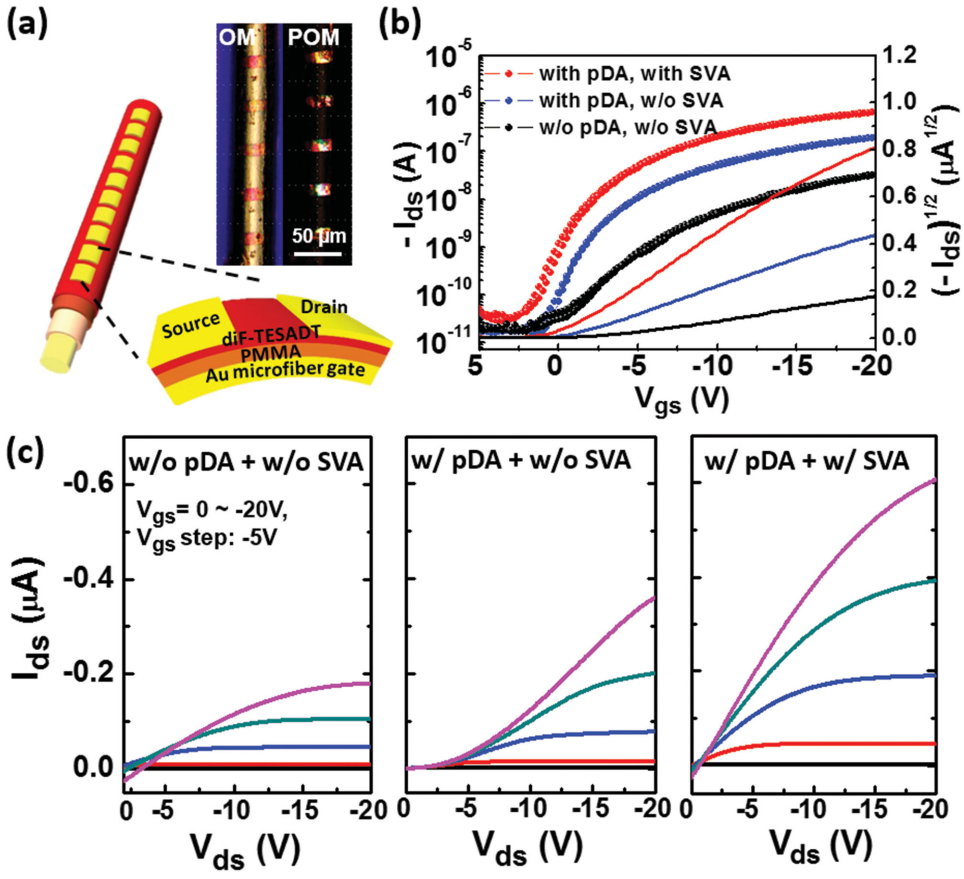


**Figure 4.** a) Schematic diagram and top-view OM image of fibriform OFET based on MIS coaxial microfiber. b) Comparison in transfer ($I_{ds}$–$V_{gs}$) characteristics (at $V_{ds}$ = −20 V) of the devices according to the pDA treatment and/or SVA. c) Output characteristics ($I_{ds}$–$V_{ds}$) of the devices according to the pDA treatment and/or SVA.

be magnified in the absence of isolation in the active layer.[20] These results verify that the MIS coaxial microfibers based on self-organization of the polymer dielectric/organic semiconductor are applicable to the FET device. Additionally, it should be noted that the proposed method is highly compatible to Cu microfiber which is low-cost material (Figure S7, Supporting Information). Through the same procedure as Au microfiber, coaxial bilayer structure of PMMA and diF-TESADT wrapping the Cu microfiber was successfully constructed, which exhibited good transistor performance with the average mobility of 0.07 ± 0.01 $cm^2\ V^{-1}\ s^{-1}$ and an $I_{on}/I_{off}$ current ratio of ≈$10^3$. Somewhat inferior electrical properties of the device based on Cu microfiber compared to that of the device based on Au microfiber might be attributed to the rough surface of Cu microfiber (Figure S8, Supporting Information).

Unlike previously demonstrated devices constructed on one side of the fiber, MIS coaxial microfibers have no directional limitation to organizing the device in the textile structure. To confirm the consistency in electrical properties over the entire fiber surface, the devices fabricated on the MIS microfiber with difference angular positioning were examined (**Figure 5**a). The OM/POM images of the four sides in Figure 5b show that the uniform phase-separation and crystallization of diF-TESADT occurred all around the MIS microfiber. As expected, the values of the charge carrier mobility (0.13 ± 0.002 $cm^2\ V^{-1}\ s^{-1}$) and on/off current ratio remained almost constant throughout all the measurement positions, as shown in Figure 5c,d. This result indicates that self-organization of diF-TESADT:PMMA blends can be a promising approach to obtain highly uniform bilayer coating on the microfiber. Furthermore, bending durability of MIS microfiber was examined (Figure 5e,f). Although a 20% decrease in mobility at the initial bending is observed, the device performance almost maintains up to 80% of the original values when the bending radius decreases down to 3.0 mm.

**Table 1.** Electrical properties for fibriform OFETs based on MIS coaxial microfibers.

| Treatment | Mobility [$cm^2\ V^{-1}\ s^{-1}$] | On/off current ratio | Threshold voltage [V] | Subthreshold swing [$V\ dec^{-1}$] |
|---|---|---|---|---|
| Without pDA Without SVA | 0.04 (±0.03) | ≈$10^3$ | −2.00 | 2.63 |
| With pDA Without SVA | 0.06 (±0.02) | ≈$10^4$ | −1.52 | 1.12 |
| With pDA With SVA | 0.19 (±0.07) | ≈$10^4$ | 0.44 | 1.28 |

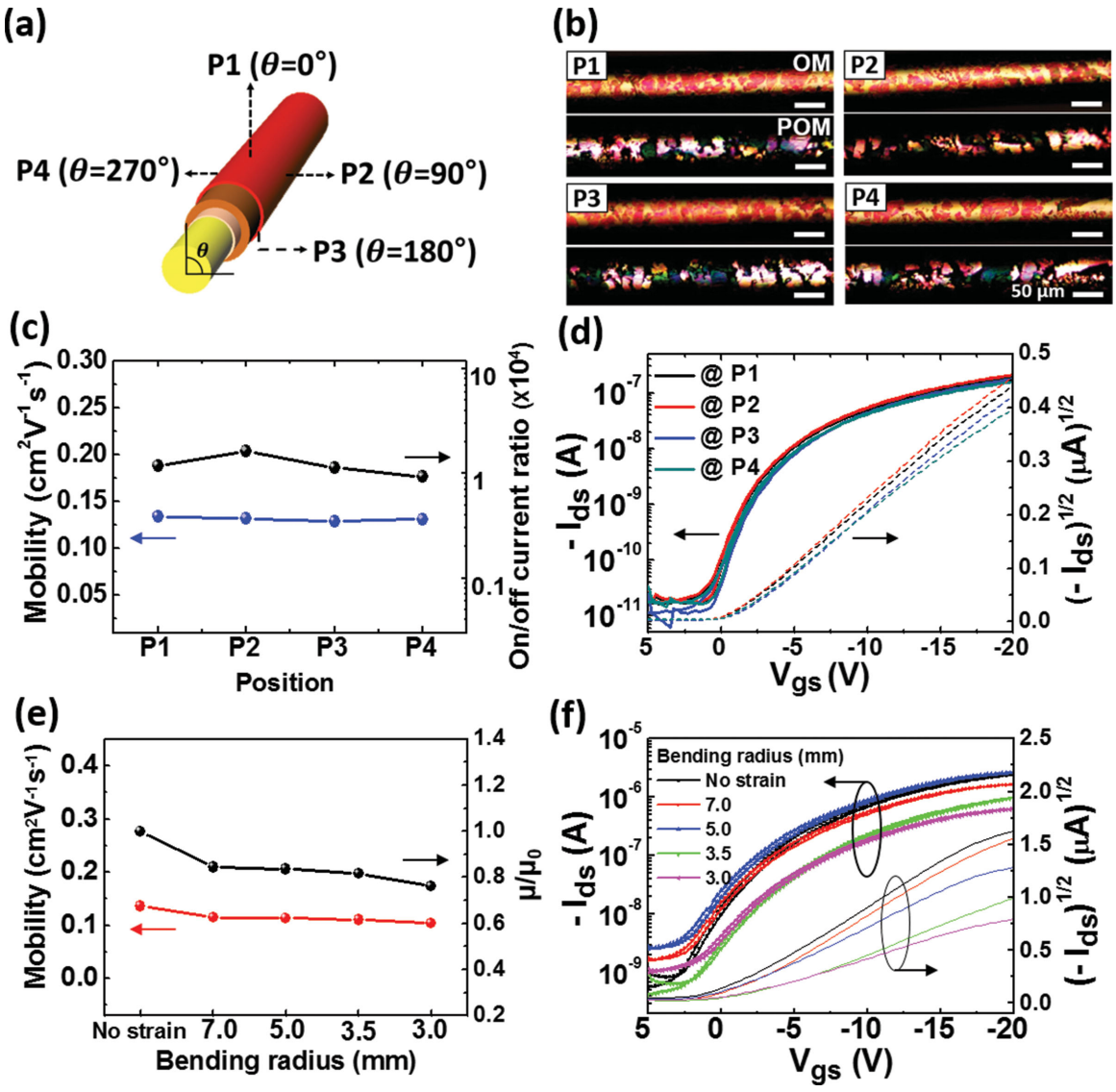


**Figure 5.** a) Schematic diagram of four side positioning at the MIS coaxial microfiber. b) OM (top)/POM (bottom) images of each position on the microfiber. c) Dependence of charge carrier mobility (left) and the current on/off ratio (right) of the devices fabricated at different positions of the MIS coaxial microfiber. d) Transfer ($I_{ds}$–$V_{gs}$) characteristics (at $V_{ds}$ = −20 V) plotted against device positions on the MIS coaxial microfiber. e) Change in carrier mobility (left) and factional mobility value in reference to initial mobility (right) at each bending radius. f) Transfer ($I_{ds}$–$V_{gs}$) characteristics (at $V_{ds}$ = −20 V) plotted against the bending radius.

Compared to previously demonstrated wire-type OFETs, which showed a critical bending radius of 10 mm,[23] the MIS coaxial-microfiber-based OFET exhibits good bending durability. Intimate contact between the gate dielectric and semiconducting layer formed by phase-separation of the polymer blend and enhanced film adhesion by the pDA treatment may be attributed to improvement of the deformation durability.

### 2.4. Prototype of Fibriform OFET-Embedded Textile

As a proof-of-concept, fibriform OFET-embedded textile was demonstrated by weaving the MIS coaxial microfiber with cotton and conducting threads (**Figure 6**a). As source (*S*) and drain (*D*) electrodes, silver-deposited conducting thread was utilized. In particular, the conducting thread was coated by conductive gel composite based on poly(3,4-ethylene dioxythiophene):polystyrene sulfonate (PEDOT:PSS) and graphene oxide (GO). It was expected that this higher work function of PEDOT/GO gel (≈5.0 eV) than Ag can induce efficient charge injection from (or to) diF-TESADT semiconductor, as well as softness of the gel composite can improve the adhesion at the contact interface between the conducting thread electrodes and the diF-TESADT semiconductor film. As shown in Figure 6b,c, the textile-embedded fibriform OFET exhibits a well-behaved gate-bias response with current levels sufficient for simple switching circuits. The field-effect mobility and on/off current ratio of the device are 0.17 $cm^2$ $V^{-1}$ $s^{-1}$ and ≈$10^3$,

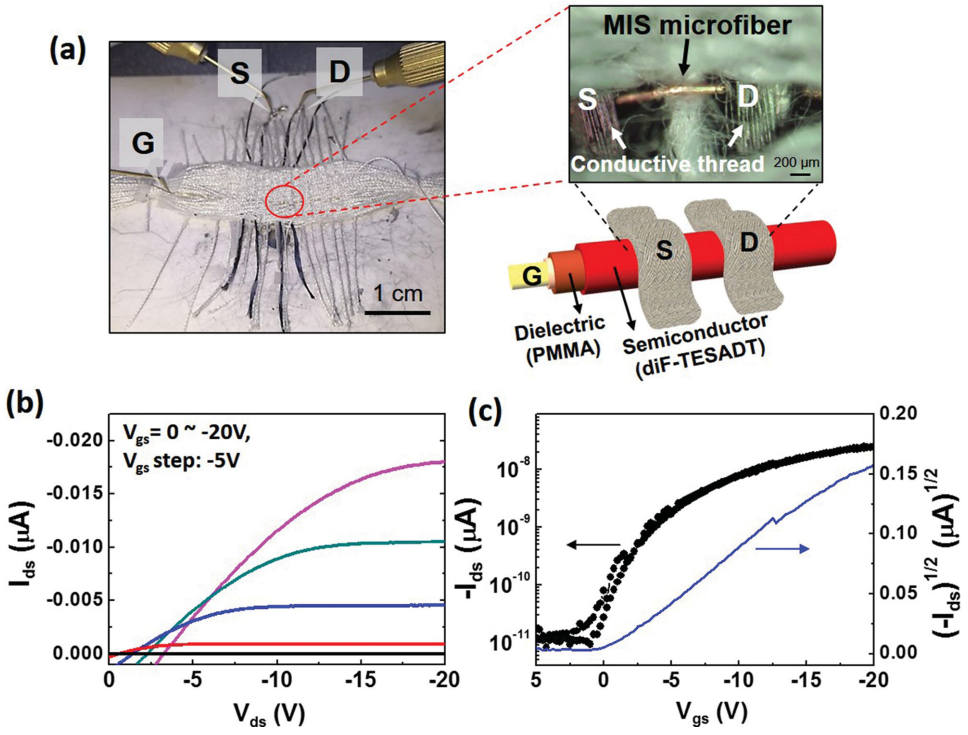


**Figure 6.** a) Photograph (left) and OM image (right) of the fibriform OFET based on MIS microfiber embedded in the textile. b) Output ($I_{ds}$–$V_{ds}$) and c) transfer ($I_{ds}$–$V_{gs}$) characteristics (at $V_{ds}$ = −20 V) of the device.

respectively. This result shows that the MIS coaxial microfiber has great potential for weaving integrated FET devices for use in wearable electronics. However, the low drain current originated from the small aspect ratio $W/L$ (i.e., channel width/length) and limited electrode contact at the thread junction remains to be improved. It is anticipated, however, that small $W/L$ may be improved by entwisting a MIS coaxial microfiber with conducting threads which act as source and drain electrodes since MIS coaxial microfiber allows to oragnize the device over the entire fiber. Further investigations regarding to this concept have been performed.

## 3. Conclusion

In this paper, we reported a metal–polymer insulator–semiconductor coaxial microfiber based on self-organization of the organic semiconductor:insulating polymer blend die-coated on metal microfiber. Vertical phase-separation of the organic semiconductor:insulating polymer blend successfully provided a bilayer structure of gate dielectric (inside) and organic semiconductor (outside) with intimate interfacial contact on the fibrous substrate. Through surface modification of the Au microfiber using polydopamine and a solvent vapor annealing process, the vertical phase-separation and crystallization of organic semiconductor molecules were significantly enhanced. We confirmed that the fibriform OFET based on MIS coaxial microfiber exhibited good electrical performance approaching the values of typical devices with planar substrate. It additionally exhibited uniformity in electrical properties over the entire fiber surface and improved bending durability. A final prototype of fibriform OFET-embedded textile was demonstrated by weaving cotton and conducting threads, which showed the feasibility of the MIS coaxial microfiber for fabricating an e-textile system for wearable electronics. Although this work focused on the diF-TESADT:PMMA blend coating on Au microfibers, the concept of one-step formation of multilayered structure on functional fibers can likely be extended to other fiber-based electronic components, such as solar cells and light-emitting diodes.[38–40] This work may therefore offer a promising strategy for preparation of electronic functional fibers and contribute to advancing progress in e-textile applications.

## 4. Experimental Section

*Materials*: PMMA, $M_w \approx 996$ kg mol$^{-1}$, dopamine hydrochloride, 1,2,4-trichlorobenzene, and 1,2-dichloroethane were purchased from Sigma–Aldrich. diF-TESADT was purchased from Lumtec. Gold microfiber with a 0.1-mm diameter (purity 99.95%) was purchased from Alfa Aesar. PEDOT:PSS was purchased from Heraeus. GO aqueous solution was purchased from Angstron Materials and freeze-dried. The GO flakes were then used. Silver-deposited conductive thread was purchased from SparkFun Electronics.

*Preparation of MIS Coaxial Microfiber*: PMMA and diF-TESADT (4:1 *w*/*w* ratio) were dissolved in 1,2,4-trichlorobenzene to generate 10 wt% solutions. Before coating of the blend solution, Au microfibers were immersed in aqueous tris-HCl buffer solution mixed with dopamine (2 mg of dopamine per ml of $10 \times 10^{-3}$ M tris-HCl, pH = 8.5) for ≈30 min. A rinse with deionized water was then followed. The treated Au microfiber was coated with a diF-TESADT:PMMA blend solution using a home-built die-coating system with a T-shaped glass tube as a reservoir, two moving stages, and a heater. The T-shaped tube with a diameter of 700 μm was filled with the diF-TESADT:PMMA blend solution by continuous feeding from a syringe. The microfiber was horizontally inserted into the tube

through the direct center and drawn at a constant speed in the horizontal direction by the moving stages. The heating unit was placed next to the tube for film drying. To induce self-organization of the diF-TESADT:PMMA blend film, the film-coated microfibers were exposed to 1,2-dichloroethane solvent vapor in a closed glass container for 2 h. The samples were dried in a vacuum oven at 60 °C overnight to remove the residual solvent.

*Device Fabrication*: To fabricate the fibriform OFETs based on the MIS microfiber, Au source and drain electrodes with a thickness of 100 nm were thermally deposited on the MIS microfiber through a transmission electron microscope grid mask. The channel width and length were 50 and 25 μm, respectively. To prepare the textile from the MIS coaxial microfiber transistors, the MIS coaxial microfibers were weaved with cotton thread and Ag-coated conductive thread, which was covered by PEDOT:GO composites using a die-coating method. The preparation of PEDOT:GO composite followed existing literature.[41]

*Characterization*: The morphologies of the coating films were observed by optical microscopy (Olympus BX51). The crystal images of the diF-TESADT were obtained with POM (Olympus BX51). SEM images of the microfiber were obtained by SEM with field effect guns (Inspect F). TOF-SIMS analysis was performed to confirm the vertical phase-separation in a blend film using TOF-SIMS 5 (ION-TOF Munster, Germany). Ion bombardment was used to slowly sputter material in an area of $100 \times 100\ \mu m^2$. The capacitance ($C_i$) of the PMMA layer sandwiched with the Au electrodes (metal–insulator–metal configuration) was determined by using an Agilent 4284A precision inductance ($L$), capacitance ($C$), and resistance ($R$) meter under ambient conditions. The electrical properties of the fibriform OFET devices were determined using an Agilent 4155B semiconductor device analyzer under ambient conditions. The calculated field-effect mobility ($\mu$) in the saturation regime was determined using the following equation $I_{ds} = \frac{WC_i}{2L}\mu\left(V_{gs} - V_{th}\right)^2$, where $C_i$ ($5.62 \times 10^{-9}$ F cm$^{-2}$) is the capacitance of the PMMA dielectric film deposited on Au microfiber, and $W$ and $L$ are the channel width and length, respectively.

## Supporting Information

Supporting Information is available from the Wiley Online Library or from the author.

## Acknowledgements

This work was supported by the Future Resource Research Program (2E25430) of the Institutional Research Program of the Korea Institute of Science and Technology (KIST).

Received: November 19, 2015
Revised: January 7, 2016
Published online: February 19, 2016

[1] Y. Meng, Y. Zhao, C. Hu, H. Cheng, Y. Hu, Z. Zhang, G. Shi, L. Qu, *Adv. Mater.* **2013**, *25*, 2326.
[2] P. Xu, T. Gu, Z. Cao, B. Wei, J. Yu, F. Li, J. H. Byun, W. Lu, Q. Li, T. W. Chou, *Adv. Energy Mater.* **2014**, *4*, 1300759.
[3] Z. Yang, J. Deng, X. Chen, J. Ren, H. Peng, *Angew. Chem., Int. Ed. Engl.* **2013**, *52*, 13453.
[4] J. Lee, H. Kwon, J. Seo, S. Shin, J. H. Koo, C. Pang, S. Son, J. H. Kim, Y. H. Jang, D. E. Kim, T. Lee, *Adv. Mater.* **2015**, *27*, 2433.
[5] S. Takamatsu, T. Kobayashi, N. Shibayama, K. Miyake, T. Itoh, *Sens. Actuators A* **2012**, *184*, 57.
[6] K. Cherenack, C. Zysset, T. Kinkeldei, N. Münzenrieder, G. Tröster, *Adv. Mater.* **2010**, *22*, 5178.
[7] W. Zeng, X. M. Tao, S. Chen, S. M. Shang, H. L. W. Chan, S. H. Choy, *Energy Environ. Sci.* **2013**, *6*, 2631.
[8] B. O'Connor, K. P. Pipe, M. Shtein, *Appl. Phys. Lett.* **2008**, *92*, 193306.
[9] Y. Zhang, W. Bai, J. Ren, W. Weng, H. Lin, Z. Zhang, H. Peng, *J. Mater. Chem. A* **2014**, *2*, 11054.
[10] Y. H. Lee, J. S. Kim, J. Noh, I. Lee, H. J. Kim, S. Choi, J. Seo, S. Jeon, T. S. Kim, J. Y. Lee, J. W. Choi, *Nano Lett.* **2013**, *13*, 5753.
[11] S. Kwon, W. Kim, H. Kim, S. Choi, B.-C. Park, S.-H. Kang, K. C. Choi, *Adv. Electron. Mater.* **2015**, *1*, 1500103.
[12] Z. Zhang, K. Guo, Y. Li, X. Li, G. Guan, H. Li, Y. Luo, F. Zhao, Q. Zhang, B. Wei, Q. Pei, H. Peng, *Nat. Photonics* **2015**, *9*, 233.
[13] Z. Zhang, Q. Zhang, K. Guo, Y. Li, X. Li, L. Wang, Y. Luo, H. Li, Y. Zhang, G. Guan, B. Wei, X. Zhu, H. Peng, *J. Mater. Chem. C* **2015**, *3*, 5621.
[14] B. O'Connor, K. H. An, Y. Zhao, K. P. Pipe, M. Shtein, *Adv. Mater.* **2007**, *19*, 3897.
[15] D. D. Rossi, *Nat. Mater.* **2007**, *6*, 328.
[16] M. Hamedi, R. Forchheimer, O. Inganas, *Nat. Mater.* **2007**, *6*, 357.
[17] C. Muller, M. Hamedi, R. Karlsson, R. Jansson, R. Marcilla, M. Hedhammar, O. Inganas, *Adv. Mater.* **2011**, *23*, 898.
[18] M. Hamedi, L. Herlogsson, X. Crispin, R. Marcilla, M. Berggren, O. Inganas, *Adv. Mater.* **2009**, *21*, 573.
[19] X. Tao, V. Koncar, C. Dufour, *J. Electrochem. Soc.* **2011**, *158*, H572.
[20] J. B. Lee, V. Subramanian, *IEEE Trans. Electron Devices* **2005**, *52*, 269.
[21] A. Bonfiglio, D. De Rossi, T. Kirstein, I. R. Locher, F. Mameli, R. Paradiso, G. Vozzi, *IEEE Trans. Inf. Technol. Biomed.* **2005**, *9*, 319.
[22] M. Maccioni, E. Orgiu, P. Cosseddu, S. Locci, A. Bonfiglio, *Appl. Phys. Lett.* **2006**, *89*, 143515.
[23] J. Jang, S. Nam, J. Hwang, J.-J. Park, J. Im, C. E. Park, J. M. Kim, *J. Mater. Chem.* **2012**, *22*, 1054.
[24] J. Granstrom, H. E. Katz, *J. Mater. Res.* **2004**, *19*, 3540.
[25] W. Zeng, L. Shu, Q. Li, S. Chen, F. Wang, X. M. Tao, *Adv. Mater.* **2014**, *26*, 5310.
[26] L. Qiu, J. A. Lim, X. Wang, W. H. Lee, M. Hwang, K. Cho, *Adv. Mater.* **2008**, *20*, 1141.
[27] W. H. Lee, J. A. Lim, D. Kwak, J. H. Cho, H. S. Lee, H. H. Choi, K. Cho, *Adv. Mater.* **2009**, *21*, 4243.
[28] S. J. Lee, Y. J. Kim, S. Y. Yeo, E. Lee, H. S. Lim, M. Kim, Y. W. Song, J. Cho, J. A. Lim, *Sci. Rep.* **2015**, *5*, 14010.
[29] H. Lee, S. M. Dellatore, W. M. Miller, P. B. Messersmith, *Science* **2007**, *318*, 426.
[30] B. H. Kim, D. H. Lee, J. Y. Kim, D. O. Shin, H. Y. Jeong, S. Hong, J. M. Yun, C. M. Koo, H. Lee, S. O. Kim, *Adv. Mater.* **2011**, *23*, 5618.
[31] D. Qúer, *Annu. Rev. Fluid. Mech.* **1999**, *31*, 347.
[32] A. Q. Shen, B. Gleason, G. H. McKinley, H. A. Stone, *Phys. Fluids* **2002**, *14*, 4055.
[33] P. Aussillous, D. Quéré, *Phys. Fluids* **2000**, *12*, 2367.
[34] W. H. Lee, D. Kwak, J. E. Anthony, H. S. Lee, H. H. Choi, D. H. Kim, S. G. Lee, K. Cho, *Adv. Funct. Mater.* **2012**, *22*, 267.
[35] W. Lee, Y. Park, *Polymers* **2014**, *6*, 1057.
[36] K. Tanaka, A. Takahara, T. Kajiyama, *Macromolecules* **1996**, *29*, 3232.
[37] S. G. Lee, H. S. Lee, S. Lee, C. W. Kim, W. H. Lee, *Org. Electron.* **2015**, *24*, 113.
[38] Z. Xu, L. M. Chen, G. Yang, C. H. Huang, J. Hou, Y. Wu, G. Li, C. S. Hsu, Y. Yang, *Adv. Funct. Mater.* **2009**, *19*, 1227.
[39] H. Y. Yang, N. S. Kang, J.-M. Hong, Y.-W. Song, T. W. Kim, J. A. Lim, *Org. Electron.* **2012**, *13*, 2688.
[40] K. H. Yim, Z. Zheng, R. H. Friend, W. T. Huck, J. S. Kim, *Adv. Funct. Mater.* **2008**, *18*, 2897.
[41] V. C. Tung, J. Kim, L. J. Cote, J. Huang, *J. Am. Chem. Soc.* **2011**, *133*, 9262.